SEA SURFACE TEMPERATURE AND WIND-GENERATED CURRENT VARIATIONS IN THE ARABIAN SEA DURING 1992 AND 1993

David Halpern
Earth and Space Sciences Division
Jet Propulsion Laboratory
California Institute of Technology
Pasadena, California 91109, U. S. A.

ABSTRACT

Monthly mean wind-generated Ekman and Sverdrup transports and the vertical transport into and out of the Ekman layer were computed from satellite scatterometer estimates of 10-m height wind speed components recorded from April 1992 to December 1993. During the summer monsoon, the Ekman southward transport was about one-half the Sverdrup southward transport, and the transport of the northward flowing Somali Current was about 30x106 $m^3 s$-l. Different results were obtained with surface wind components produced at a numerical weather prediction center, illustrating the sensitivity of results to the wind data product. A correlative relationship is found between the May-to-August decrease of sea surface temperature over the Arabian Sea and the Ekman southward transport out of the Arabian Sea and the vertical transport of water into the Ekman layer in the Arabian Sea.

1 INTRODUCTION

Two remarkable phenomenon occur in the Arabian Sea, defined as the North Indian Ocean region north of 8°N and west of India. The sea surface temperature (SST) in August (summer time) is nearly as low as that in January and February (winter time). The surface wind speed is largest in July, actually twice as large as in January or February. Both features are very different than those found in the annual cycles of SST and surface wind speed at similar latitudes in other oceans.

Many processes influence SST in the Arabian Sea: clouds, wind mixing, horizontal and vertical heat advection, and air-sea heat fluxes. This brief report describes a search for correspondence between variations of monthly mean SST and wind-driven currents in the Arabian Sea during April 1992 and December 1993.

The monthly mean average SST over the Arabian Sea reached maximum values in May (Figure 1A). The Gulf of Aden and the Gulf of Oman were not included in the analysis. The SST is almost uniform throughout the Arabian Sea in May, with horizontal variations less than 2 “C (Figure 1B). In 1992 and 1993, the average SST in the Arabian Sea decreased by 3 ‘C from May to August (Figure 1A). The cooling was not uniform over the Arabian Sea because the SST dropped 4-5 °C in the western Arabian Sea and 2 °C in the eastern Arabian Sea (Figure 1 C). In August, the predominant north-south pattern of the 26 “C isotherm near 60°E (Figure 1C) is suggestive of processes that lower SST that are not related to solar radiation, in contrast to the east-west patterns of the 29 and 30 ‘C isotherms that occurred in May (Figure 1 B). The hypothesis to be tested is that SST is lowered when warm upper-layer water escapes southward and upper-layer water is cooled by upward advection of subsurface water. Whether wind-driven horizontal and vertical currents have a correspondence with SST variations will be examined.

The June-September All-India Rainfall Index was 7% below normal in 1992 and 2% above normal in 1993 (J. Shukla, personal communication, 1994), which represents a year-to-year change of nearly 10%. In May the average SST over the Arabian Sea was about 0.2 ‘C larger in

1993 than in 1992 (Figure 1A). Whether higher amount of rainfall was related to higher SST, which could be expected to occur because of increased evaporation associated with higher SST, is not known because many factors contribute to monsoon rainfall over India. However, the relationship between Arabian Sea SST and India rainfall seems to be weak because the substantial 35% change in the All-India Rainfall Index from 1987 to 1988, which was the largest year-to-year change in nearly 70 years, was associated with the June 1987 to June 1988 SST variation in the Arabian Sea of about 0.5 "C (World Meteorological Organization, 1992).

2 DATA

Monthly mean 2° x 2° averaged SST values (Reynolds, 1988) were obtained electronically y from the Coupled Model Project (CMP), National Meteorological Center (NMC), National Oceanic and Atmospheric Administration (NOAA). The SST data product combines in situ observations with advanced very high resolution radiometer (AVHRR) retrievals from NOAA polar-orbiting spacecraft. The root-mean-square (rms) accuracy of near-instantaneous SST values is about 0.8 "C (Reynolds, 1988).

Monthly mean 1° x 1° averaged wind components at 10-m height were computed from the Freilich and Dunbar (1993) wind data product (called CMODFD [Q-band model Freilich and Dunbar]) derived from electromagnetic radiation measurements recorded by the European Space Agency (ESA) first Earth Remote Sensing (ERS- 1) satellite. Therms accuracy of monthly mean CMODFD wind components is about 1.0 m s^{-1} (Halpern et al., 1994).

3 WIND-DRIVEN CURRENT

3.1 Horizontal Current

The Ekman (1905) or wind-driven current for an idealized ocean that is homogeneous in density, infinite in depth, boundless in horizontal extent, and for an idealized wind that is uniform in horizontal direction and constant in time is confined to a shallow near-surface layer of approximately 50-100 m thick. Current speed decreases exponentially with depth and the direction rotates clockwise in the northern hemisphere (counterclockwise in the southern hemisphere). The east-west and north-south Ekman current transport components per unit width are M^E_x [m^2 S-l] = $\tau_y/\rho f$ and M^E_y [$m^2 s^{-1}$] = - $\tau_x/\rho f$, respectively, where τ_x and τ_y are the zonal and meridional components of surface wind stress, respectively, p is water density, and f is the Coriolis parameter which is zero at the equator. Positive directions of τ_x and τ_y are eastward and northward, respectively. Daily wind stress components were computed from daily 1° x 10 wind speed components, according to the square-law formulation and wind-speed dependent drag coefficient described by Trenberth et al. (1990). Monthly mean 10 x 10 wind stress components were equal to calendar-month arithmetic mean values. Maximum monthly mean surface wind stress magnitudes occurred in July, and the wind stresses in July 1993 were slightly more intense than those in July 1992. The July 1993 wind stress and wind-stress curl (curl $\tau = \partial\tau_y/\partial x - \partial\tau_x/\partial y$), which is employed in the calculation of wind-driven currents, is shown in Figures 2A and 2B, respectively.

The total monthly north-south Ekman transport along a latitude, called ET_y, exhibited a strong annual cycle during 1992 and 1993 over nearly the entire Arabian Sea (except in the far northern region north of 20"N where the magnitude was small), with southward direction from May to November and northward direction the remainder of the year (Figure 3A). At a specific latitude, the maximum southward transport was greater that the maximum northward transport. During the 1992 and 1993 summer monsoons, the ET_y values were similar, Latitude-time variations in 1992 were very similar to those in 1993.

The wind-driven vertically integrated north-south transport per unit width [$m^2 s^{-1}$] between the surface and an arbitrary depth of no motion (say, at 2000 m) is equal to curl $\tau/\rho\beta$ and is called the Sverdrup (1947) transport. Beta, β, is the latitudinal change of the Coriolis parameter. The total monthly Sverdrup transport along a latitude (Figure 3B) exhibited a strong annual cycle, like ET_y, but only south of 13"N did the Sverdrup transport direction alternate between northward and southward (Figure 3B). During the summer monsoons of 1992 and 1993, the Sverdrup transports were southward below 13"N and northward above 13"N. North of 13"N, the maximum northward total Sverdrup transport was maximum in July during the summer monsoon. During the summer monsoon, the largest north-south gradient of Sverdrup southward transports occurred between 8°'N and 13"N, and the gradient was more intense in 1993 than in 1992. South of 13"N the directions of the Sverdrup and meridional Ekman transports were the approximately same (Figures 3A and 3B).

3.2 Vertical Current

The wind-driven Ekman currents are horizontally nondivergent, resulting in vertical motion into or out of the Ekman layer. The vertical velocity per unit area, W_E [m S-l], is equal to $(1/\rho f)$ (curl $\tau + \beta\tau_x/f$) (Stommel, 1965). The total monthly vertical transport across an area of the Ekman layer defined by the distance along a latitude and a one-degree north-south distance is shown in Figure 3C. During the southwest monsoon, the vertical transport was upwards throughout the Arabian Sea, except south of 10"N. The Gulf of Aden and the Gulf of Oman were not included in the analysis. Downward transports occurred primarily south of 10"N during the summer (July) and winter (January) monsoons. Year-to-year variations were small.

4 RESULTS

The total wind-driven transports along 8.5°N, which is less than 50 km north of the southernmost latitude of India, will be discussed. North of 8.5°N the Arabian Sea is essentially a closed basin, with the Gulf of Aden and the Gulf of Oman not included in the analysis.

During the southwest monsoon months of June and July, the southward Ekman and Sverdrup transports reached maximum values of about 23 Sv (1 Sv = 1 $x10^6$ $m^3 s^{-1}$) and 12 SV, respectively, and at the same time the vertical transport into the Ekman layer was maximum at about 6 Sv (Figure 4). Consistent with the Ekman southward transport and upward motion (i. e., Ekman suction) during the summer monsoon were the Ekman northward transport and Ekman pumping (i. e., Ekman pumping) that occurred during the northeast monsoon during winter months (Figure 4).

That the magnitude of the Ekman southward transport was greater than the volume of water transported into the Ekman layer during the summer monsoon indicated the occurrence of an additional source of upper-layer water flowing into the Arabian Sea. The major source of northward transport into the Arabian Sea is the Somali Current, which is a narrow-width western boundary current. According to our estimates of wind-driven currents, the transport of the Somali Current, which ought to equal the sum of the upward transport into the Arabian Sea and Sverdrup transport, was about 30 Sv. This value is similar to the observed Somali Current transport at 10°N during the southwest monsoon (Bruce *et al.*, 1994).

In May when SST reached its maximum value in the Arabian Sea (Figure 1A), the vertical exchange of water between the Ekman layer and deeper water and the north-south component of the Ekman transport were negligible (Figure 4), In June when SST began to decrease (Figure 1A), the average vertical velocity throughout the Arabian Sea was upward and the Ekman meridional transport was southward along the southern boundary of the Arabian Sea (Figure 4). Ekman suction into the near-surface layer and Ekman transport outflow from the Arabian Sea continued

during July and August, but the magnitudes of the transports diminished (Figure 4). The average SST over the Arabian Sea reached a relative minimum in August; the absolute minimum SST occurred in January and February (Figure 1A), as expected of locations in the northern hemisphere. The increased SST in September compared to August, albeit less than 0.25 "C (Figure 1A), was associated with continued Ekman suction and southward transport, both of which had small magnitudes, indicating that solar radiative heating and other processes had a more important influence upon SST than wind-driven horizontal and vertical currents.

5 CONCLUS1ONS

Nearly two years of ERS-1 CMODFD scatterometer wind data showed that monthly mean variations of vertical transport into the Ekman layer and Ekman southward transport were in phase with the SST decrease associated with the southwest monsoon. The relative importance of other processes that reduce SST need investigation, such as clouds, evaporation, and wind-generated mixing which entrains thermocline water into the surface mixed layer.

Wind-driven currents are, obviously, dependent on the wind field, and there exist many surface wind data and data products for 1992 and 1993. In the case of the ERS-1 scatterometer, the CMODFD data is only one of several ERS-1 scatterometer data products. The wind-product sensitivity of the computed wind-driven horizontal and vertical transports in the Arabian Sea is examined by comparison of results derived from the 10-m height surface wind components computed at 12 hour intervals on a 2.5° x 2.5° grid by the European Centre for Medium-Range Weather Forecasts (ECMWF). Comparison of Figures 4 and 5 reveal that seasonal variations of monthly mean CMODFD and ECMWF total upward transports into the Ekman layer throughout the Arabian Sea were similar, but the maximum ECMWF upward transport was twice as large as that computed with CMODFD data. As already noted, during the summer monsoon the CMODFD-derived Ekman southward transport was one-half the magnitude of the Sverdrup southward transport along 8.5°N (Figure 4). However, the ECMWF data product yielded the opposite conclusion along 8.75°N: the Ekman southward transport was nearly two times larger than the Sverdrup southward transport (Figure S). A consequence of the ECMWF wind-driven southward transports is that a northward transport beneath the Ekman layer of at least 10 Sv enters the Arabian Sea along 8.75°N. In the case of the ECMWF data product, the computed Somali Current transport would be 20 Sv, which is about two-thirds the magnitude estimated from the CMODFD wind-driven currents.

6 ACKNOWLEDGEMENTS

I am indebted to Dr. Michael Freilich, Oregon State University, and Dr. Scott Dunbar, JPL, for creating and distributing a value-added ERS-1 surface wind data product. Dr. Richard Reynolds, NOAA, kindly made available the blended SST analysis. The ECMWF data product was obtained from ECMWF. William Knauss, JPL, ably kept track of millions of numbers, various data sets, and produced the diagrams in his usual proficient manner. Support by the NASA Earth Observing System (EOS) SeaWinds Project and by NASA RTOP 578-22-26 is gratefully acknowledged. The research described in this paper was performed by the Jet Propulsion Laboratory, California Institute of Technology, under contract with the National Aeronautics and Space Administration

7 REFERENCES

Bruce, J. G., D. R. Johnson and J. C. Kindle, 1994: Evidence for eddy formation in the eastern Arabian Sea during the northeast monsoon. J. Geophys. Res., 99,7651-7664.

Ekman, F. W., 1905: On the influence of the earth's rotation on ocean-currents. Arkiv Mater n., Astr. Fysik, Bd 2, No. 11, 53 pp.

Freilich, M. H. and R. S. Dunbar, 1993: A preliminary C-band scatterometer model function for the ERS-1 AMI instrument. In, Proceedings First ERS - 1 Symposium, ESA SP-359, European Space Agency, Paris, 79-84.

Halpern, D. , M. H. Freilich and R, S. Dunbar, 1994: ERS- 1 scatterometer estimates of annual variations of Atlantic ITCZ and Pacific NECC. In, Proceedings Second ERS- 1 Symposium, ESA SP-361, European Space Agency, Paris, 1003-1008.

Reynolds, R. W., 1988: A real-time global sea surface temperature analysis. J. Clim., 1,75-86.

Stommel, H. M., 1965: The Gulf Stream. Univ. California Press, Berkeley, 248 pp.

Sverdrup, H, U., 1947: Wind-driven currents in a baroclinic ocean; with application to the equatorial currents of the eastern Pacific. Proc. Nat. Acad. Sci Wash., 33,318-326.

Trenberth, K, E., W. G. Large and J. G. Olson, 1990: The mean annual cycle in global ocean wind stress. J. Phys. Oceanog., 20, 1742-1760.

World Meteorological Organization, 1992: Simulation of interannual and intraseasonal monsoon variability. WCRP-68, WMO/TD-470, World Meteorological Organization, Geneva.

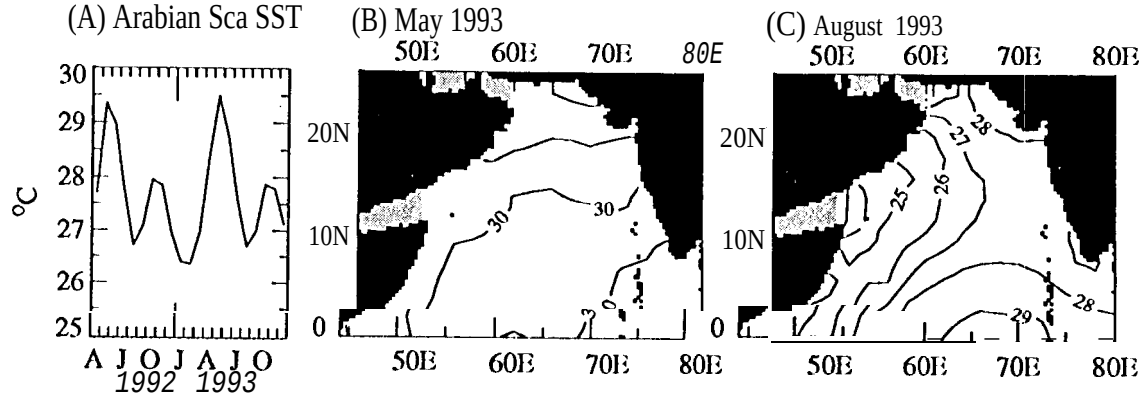

Figure 1. (A) Time series of monthly mean sea surface temperature (SST) in the Arabian Sea (without the Gulf of Aden and Gulf of Oman) computed from Reynolds (1988) monthly mean 2° x 2° SST data product. (B) May 1993 SST distribution. (C) August 1993 SST distribution.

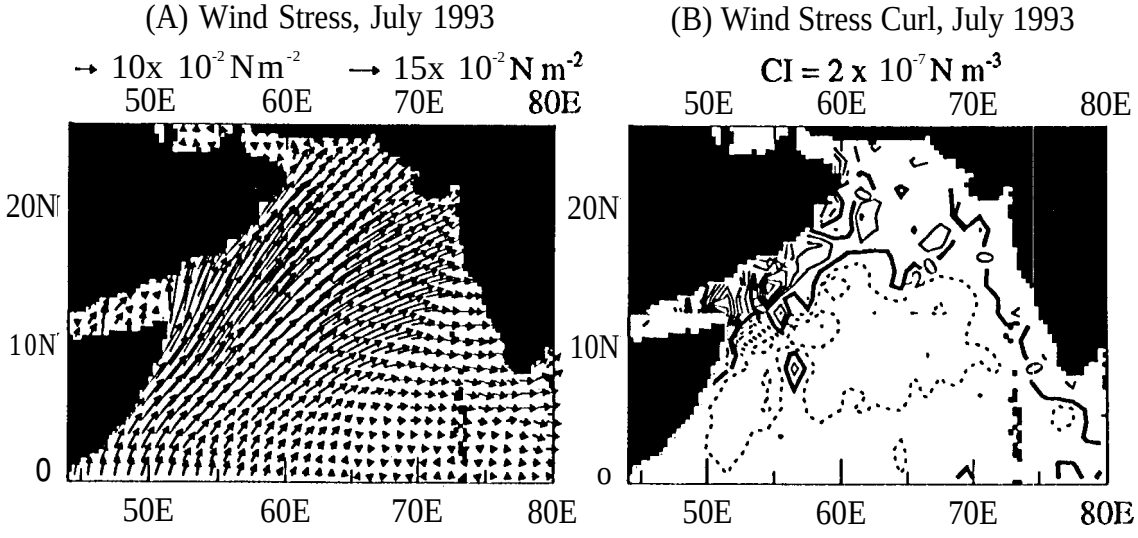

Figure 2. (A) Monthly mean July 1993 surface wind stress distribution computed from the Freilich and Dunbar (1993) CMODFD ERS-1 scatterometer wind data product. (B) Monthly mean July 1993 wind stress curl computed from (A).

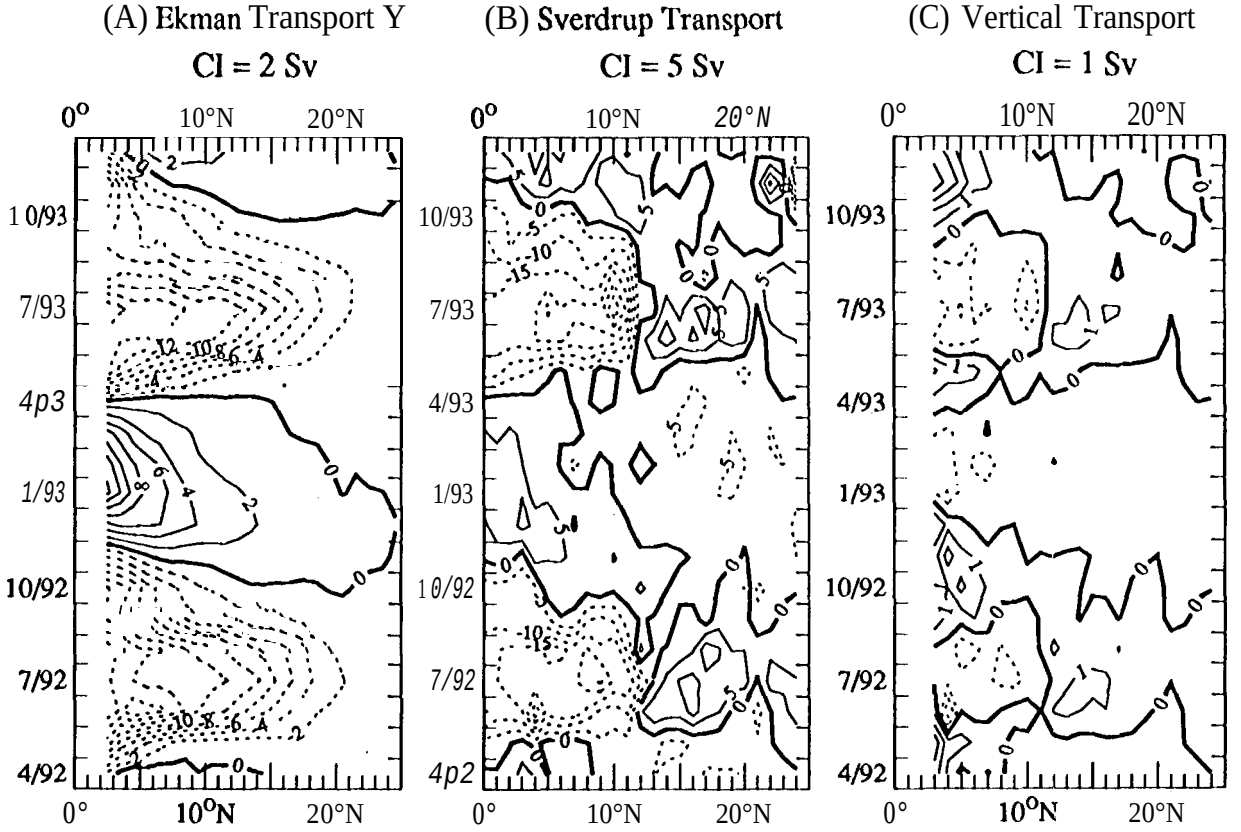

Figure 3. (A) Time series of the monthly mean total north-south component of Ekman transport (Sv) along a latitude. A solid contour indicates a positive value, in which the direction is northward. South of India, the westernmost longitude was 78°W. (B) Time series of the monthly mean total Sverdrup transport (Sv) along a latitude. A solid contour indicates a positive value, in which the direction is northward. South of India, the westernmost longitude was 79°W. (C) Time series of the monthly mean total vertical transport (Sv) into or out of the Ekman layer along a latitude and a lo-latitudinal distance. A solid contour indicates a positive value, in which the direction is upwards. South of India, the westernmost longitude was 79°W. In each case, the contour interval , CI, is displayed at the top of each panel. CMODFD data product was used.

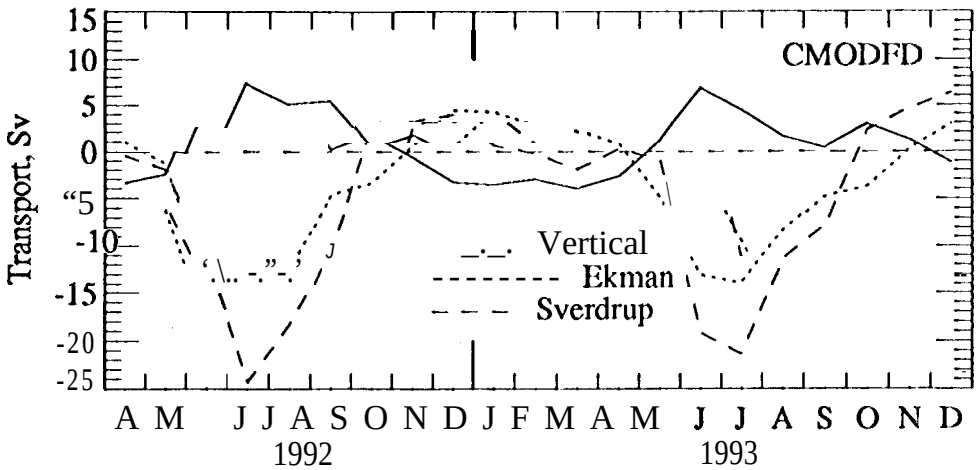

Figure 4. Time series of monthly mean (a) total vertical transport (solid line) into (positive values) or out of the Ekman layer of the Arabian Sea (without the Gulf of Aden and Gulf of Oman), (b) north-south component of the Ekman transport (dotted line) across 8.5°N (positive values mean towards the north), and (c) Sverdrup transport (dash line) across 8.5°N (positive values mean towards the north). CMODFD data product was used,

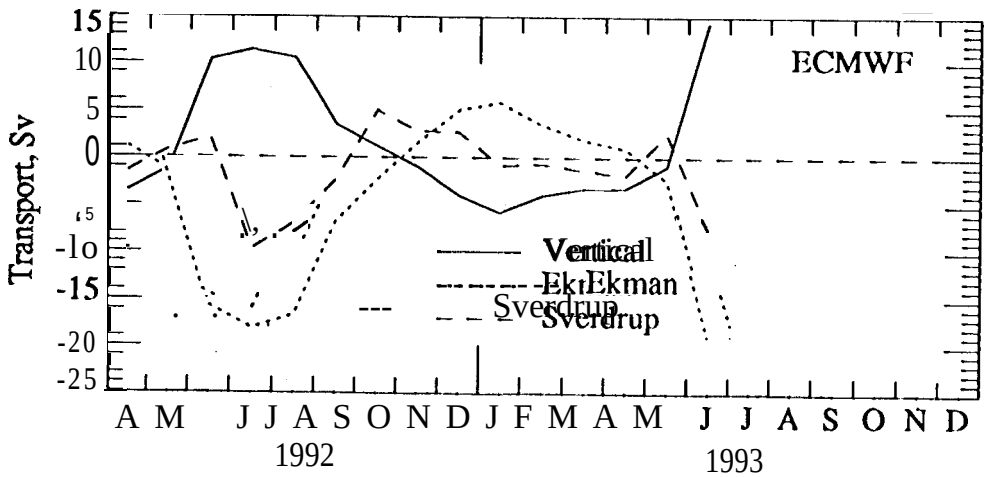

Figure 5. Same as Figure 4, except ECMWF data product was used.